Ambient wind energy harvesting using cross-flow fluttering

Shuguang Li,[1,2,a)] Jianping Yuan,[1] and Hod Lipson[2,b)]
[1]*College of Astronautics, Northwestern Polytechnical University, Xi'an, Shaanxi, 710072, People's Republic of China*
[2]*Sibley School of Mechanical and Aerospace Engineering, Cornell University, Ithaca, New York 14853, USA*

(Received 26 July 2010; accepted 6 November 2010; published online 27 January 2011)

In this experimental study, we propose and test a bioinspired piezo-leaf architecture which converts wind energy into electrical energy by wind-induced fluttering motion. While conventional fluttering devices are arranged in parallel with the flow direction, here we explore a dangling cross-flow stalk arrangement. This architecture amplifies the vibration by an order of magnitude, making it appropriate for low-cost organic piezomaterials. We fabricated prototypes using flexible piezoelectric materials as stalks and polymer film as leaves. A series of experiments demonstrated a peak output power of approximately 600 μW and maximum power density of approximately 2 mW/cm^3 from a single leaf. © *2011 American Institute of Physics*. [doi:10.1063/1.3525045]

Solid-state wind vibration devices can harvest energy from ambient wind flows by exploiting fluttering phenomena. Such devices have the potential to extract energy from low velocity, irregular flows, at considerably small volumes. The key challenge in designing such fluttering energy harvesters is to reach a power density and cost effectiveness that approaches that of a conventional wind turbine. Most conventional architectures, such as the parallel-flow stalk-leaf design shown in Fig. 1(a), are still orders of magnitude away from reaching this goal. Extensive works have focused on using piezoelectric materials to convert mechanical vibration energy into electrical power.[1–10] A brief overview of related works is provided in the supplementary materials.[11]

In this paper, we attempt to harvest the wind-induced mechanical vibration energy using an untensioned, free-edge cross-flow arrangement compatible with polymer piezoelectric materials. We chose a flexible and robust piezoelectric material (PVDF) as an essential component of device to allow for a wide range of fluttering frequencies. In our prototype,[11] the flexible leaf structure is driven to oscillate like a leaf flapping in the wind. This flapping is attributed to instability in the aeroelastic system. Two potential excitations may be responsible for the unstable periodic motion of a flexible body. Classical studies predict that the dominant exciter of this oscillation phenomenon is vortex shedding from the bluff body.[12,13] Most recent work, however, has ignored or idealized the effect of a bluff body at the leading edge, paying more attention to the self-induced aerodynamic instability of the trailing edge.[14–19]

Our exploratory experimental studies have shown that a cross-flow stalk configuration produced significantly more power than a parallel-flow configuration, even without a bluff body.[20] This observation indicates that the self-induced vibration of the trailing edge played the main role in our experiments. The interactions between the coupled bending-torsion deformation and the aerodynamic load have the potential to trigger a much stronger flutter motion. As for the driving mechanism, the horizontal-stalk leaf is driven by the pressure difference between the two sides of leaf, and this pressure is induced by vortex shedding from the leading edge (bluff body) and/or the tailing edge. This kind of vibration is considered as the typical vortex-induced vibration (VIV).[12] In contrast, at the beginning of vibration, the vertical-stalk leaf is driven by the vortex shedding from the leaf's training edge, this typical VIV could lead a small torsion and bending of the stalk. This coupled bending and torsion deformation then induces an attack angle and sideslip angle between the harvesters and the airflow. These two angles further result in aerodynamic lift and sideslip forces that eventually trigger the flutter motion. We believe that this flutter is a form of self-excited (self-induced) vibration. During flutter, the deformation/movement of the object increases an aerodynamic load which in turn drives the object to deform/move further. This process continues until it approaches dynamic stability with a large-amplitude vibration.

For the cross-flow stalk-leaf generator [Fig. 1(b)],[11] the direction of the leaf is no longer the same as stalk, but still in the direction of the airflow. The device thus looks more like an "L" shape. In this configuration, the stalk twists as well as bends. We consider a simplified model of the coupled fluid-structure system which is abstractly treated as an aerodynamic-instability driven cantilever-pendulum system. Such a system can act as either an absorber or an amplifier of

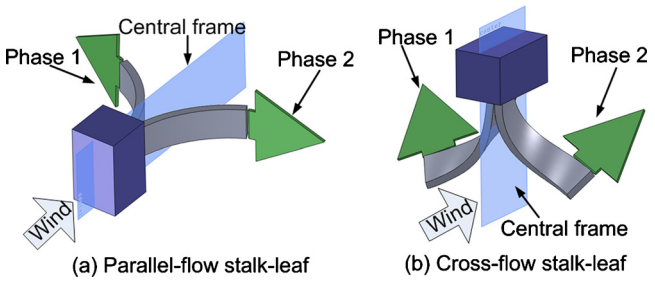

FIG. 1. (Color online) Motion sketch of two different structures: (a) parallel-flow stalk-leaf. (b) Cross-flow stalk-leaf.

a)Electronic mail: lisg81@gmail.com.
b)Electronic mail: hod.lipson@cornell.edu.

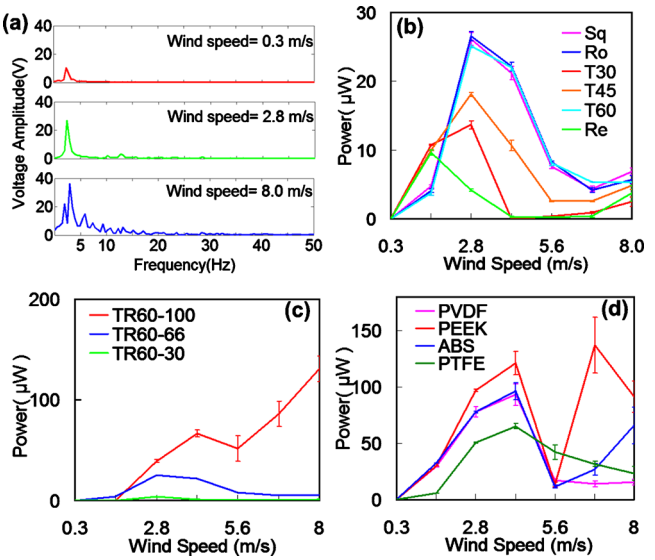

FIG. 2. (Color online) Leaf performance: (a) typical wind response of piezo-leaf's output, where the top plot is a bistable status, middle one has single stable status, and the plot at the bottom is a chaotic multiple modals oscillation/bistable response. (b) Output power on different shapes of leaf with same materials (PVDF with 0.01 in. thickness) and area(14.4 cm^2), where Sq, Ro, T30, T45, T60, and Re denote the shape of square, round, isosceles triangle (30° base angle), isosceles triangle (45° base angle), equilateral triangle, and rectangle (7.2×2 cm^2), respectively. (c) Output power on same materials (PVDF with 0.01″ thickness) and shapes (equilateral triangle) of leaf but different areas where TR60-100, TR60-66, and TR60-30 represent the hemline's length on 10 cm, 6.6 cm, 3 cm, respectively. (d) Different materials' output power using same shape (equilateral triangle) and area (hemline=10 cm). All loads were 10 MΩ.

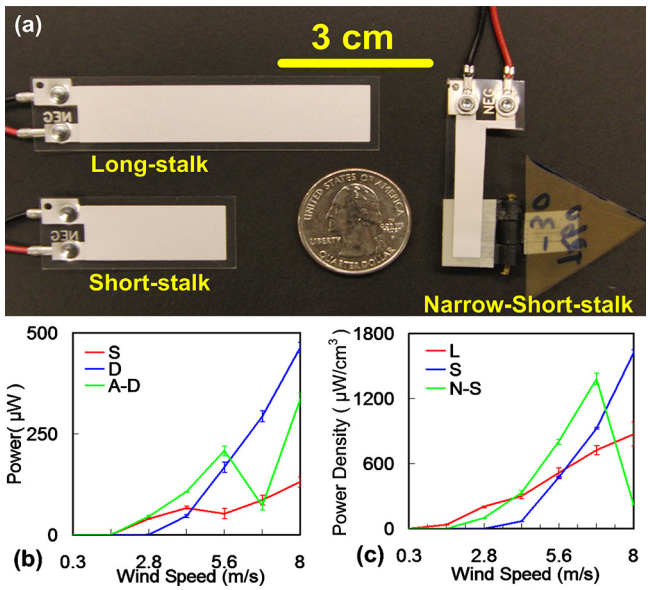

FIG. 3. (Color online) Stalk performance: (a) Three scales of PVDF stalk used in experiments, long stalk, short stalk, and narrow-short stalk, all stalk thickness are 205 μm. (b) Output power on different stalk configurations, where S, D, and A–D denote the single-layer, adhered double-layer, and air-spaced double-layer, respectively. (c) Density of output power on different scales of stalk, where L, S, and N–S represent long, short, and narrow-short stalk, respectively. All loads were 10 MΩ.

vibration depending on the parametric conditions.[21–24]

While an analytical model for a combined torsion and bending aeroelastic system is beyond the scope of this paper, we discuss a series of experiments conducted to investigate the system properties. All experiments were performed in a small wind tunnel (cross-section: 25×25 cm^2). The experimental wind speed range was 0–8 m/s, measured using a small digital wind meter (WindMate 200; Speedtech Instruments). We recorded the output voltage using digital oscilloscopes (DSO6014A; Agilent Technologies). The root-mean-square of voltage V_{rms} was measured over a period of approximately 2 s through the X10 probe (10 MΩ). The average output power P_o was calculated using the following relationship:

$$P_o = \frac{(V_{rms})^2}{R}. \quad (1)$$

As Fig. 2(a) shows, a bistable response was observed. There exists a critical speed region where the coupled systems either stays flat or periodically bursts into large-amplitude oscillations; if the wind speed is beyond the critical region and gets into the single-stable region, the leaf will flap in a periodic large-amplitude; finally, over the stable region, a chaotic multiple-modal oscillation, or even another bistable response will appear occasionally. This classical fluid-induced bistable and chaotic phenomenon was frequently observed in previous studies.[18,19,25]

The output power level is sensitive to the leaf's shape [see Fig. 2(b)]. In this comparison we used the same materials with identical thicknesses and areas but with different symmetric geometric shapes. The results reveal that the circle, square, and equilateral triangle have similar performance. We conclude that the shapes' moment of inertia relative to the hinge's rotational axis may be a key aspect of the leaf design.

The plots seen in Fig. 2(c) show two trends of the wind response. First, as the area increases, the cut-in speed (critical speed) becomes higher. Second, the peak power value increases with increasing area. A larger leaf area can harvest more energy from airflow but the increased mass requires a higher wind speed to approach the critical flapping condition. A simplified model of this coupled aeroelastic system allows us to understand these experimental results from an energy perspective.[11]

A potential way to extract higher output is to use multiple PVDF elements to get more output power from a single device. However, there exists a fundamental tradeoff between increased strain and added stiffness of a multilayer stalk. From Fig. 3(b), we can easily see the difference between single and double-layer designs. Generally, both double-layer devices produce higher power than the single-layer device; however, in addition to a narrowed wind speed response band, they need a higher cut-in wind speed to get into large-amplitude oscillation. We further found an air-spaced double-layer configuration to be a good compromise with a low cut-in wind speed and a high average output power. Moreover, the double-layer stalk showed a higher peak value in a high speed wind. A similar experiment was also shown by Wang *et al.*[26]

In order to approach a higher power density, defined as power value divided by stalk's volume (microwatt per cubic centimeter), we tested three different dimensions of PVDF stalks. The narrow-short stalk was cut to half width of the short stalk using a sharp metal blade [Fig. 3(a)]. As the plots

TABLE I. Power density comparison of wind energy harvesting devices.

Device	Configuration	Dimension (mm)	Peak power	Power density: Per weight (mW/kg)	Power density: Per volume (mW/cm^3)	Power density: Per swept area (W/m^2)	Power density: Per cost (mW/U.S.$)	Cut-in speed (m/s)
Small windmill	Bimorph	60×20×0.6	5 mW	77.2	0.579	0.13	0.021	2.4
Galloping beam	Bimorph	100×38×1.54	1.14 mW	74	0.556	Unknown	Unknown	2.5
Windbelt (micro)			5 mW	Unknown	Unknown	1.28	Unknown	2.7
Tan's harvester	Bimorph	76.7×12.7×2.2	0.16 mW	9.94	0.075	Unknown	Unknown	~3
Flaglike harvester	Bimorph	203×279×0.5	10 mW	Unknown	0.347	Unknown	0.033	~4.5
Devices presented in this paper								
Parallel-flow long stalk	Unimorph	72×16×0.205	0.02 mW	34	0.09	0.001	0.003	1.5
Cross-flow long stalk	Unimorph	72×16×0.205	0.21 mW	343	0.871	0.013	0.034	1.5
Cross-flow short stalk	Unimorph	41×16×0.205	0.26 mW	576	1.928	0.046	0.069	4
Cross-flow double-layer long stalk	Bimorph	72×16×0.41	0.61 mW	472	1.300	0.039	0.051	4
Cross-flow narrow-short stalk	Unimorph	41×8×0.205	0.14 mW	415	2.036	0.024	0.037	2.8
Typical commercial wind turbine								
VESTAS V52-850KW			850 kW	27 000	Unknown	400	~300	4

of Fig. 3(c) show, for the low speed region (under 4 m/s), the long stalk has the highest power density, while in medium wind speeds (4–7.5 m/s), the narrow-short stalk takes the leads. However, when the wind speed exceeds 7.5 m/s, the short stalk achieves the highest power density. These trends can be attributed to the tradeoff between the reduced length (width) and increased bending stiffness.

When measuring power, the load can greatly affect the results. Previous research has suggested an optimized matching resistance for determining the output power of piezoelectric vibration generators.[5,27,28] Thus, we chose the best resistance for our device in order to obtain the peak power and power density.[11] We observed a peak power of approximately 615 μW for an adhered double-layer stalk in 8 m/s wind on 5 MΩ load. The maximum power density was approximately 2036 μW/cm^3 for a narrow-short stalk in 7 m/s wind under a 30 MΩ load. Compared to other piezomaterials based wind energy harvesters, our devices show excellent performance in power normalized by weight, volume, and cost (Table I). However, our devices compare less favorably in power per swept area. We should note that the swept area performance of our devices could be improved by stacking multiple devices behind one another. Additionally, it is likely that the complex flexing dynamics cause various regions of the piezomaterial to cancel their output both longitudinally and transversally. This would imply that even greater performance could be expected from future designs with segmented electrodes or patterned poling.

In conclusion, while commercial wind turbines lead piezomaterials wind energy harvesters in power density, efficiency, and capacity, fluttering harvesting devices have potential advantages in compactness, robustness, and simple construction. The dangling cross-flow architecture proposed here could help to diminish this performance gap and make solid-state wind energy harvesting a more viable alternative.

This research was sponsored by the Cornell Center for a Sustainable Future and the Chinese Scholarship Council. We thank Professors Francis C. Moon, Charles H. K. Williamson, and Ephrahim Garcia of Cornell University and their students for help with wind tunnel tests and experimental advice.

[1] S. R. Anton and H. A. Sodano, Smart Mater. Struct. **16**, R1 (2007).
[2] J. A. Paradiso and T. Starner, IEEE Pervasive Comput. **4**, 18 (2005).
[3] H. A. Sodano, D. J. Inman, and G. Park, Shock Vib. Dig. **36**, 197 (2004).
[4] S. P. Beeby, M. J. Tudor, and N. M. White, Meas. Sci. Technol. **17**, R175 (2006).
[5] S. Priya, J. Electroceram. **19**, 167 (2007).
[6] S. Roundy, P. K. Wright, and J. Rabaey, Comput. Commun. **26**, 1131 (2003).
[7] D. Shen, S. Choe, and D. Kim, Jpn. J. Appl. Phys., Part 1 **46**, 6755 (2007).
[8] H. A. Sodano, G. Park, and D. J. Inman, Strain **40**, 49 (2004).
[9] A. Erturk, J. Hoffmann, and D. J. Inman, Appl. Phys. Lett. **94**, 254102 (2009).
[10] F. C. Moon and P. J. Holmes, J. Sound Vib. **65**, 275 (1979).
[11] See supplementary material at http://dx.doi.org/10.1063/1.3525045 for calculation and experiment details.
[12] C. H. K. Williamson and R. Govardhan, Annu. Rev. Fluid Mech. **36**, 413 (2004).
[13] S. Shukla, R. N. Govardhan, and J. H. Arakeria, J. Fluids Struct. **25**, 713 (2009).
[14] L. Huang, J. Fluids Struct. **15**, 127 (1995).
[15] M. Argentina and L. Mahadevan, Proc. Natl. Acad. Sci. U.S.A. **102**, 1829 (2005).
[16] L. Tang and M. P. Païdoussis, J. Sound Vib. **305**, 97 (2007).
[17] C. Eloy, C. Souilliez, and L. Schouveiler, J. Fluids Struct. **23**, 904 (2007).
[18] J. Zhang, S. Childress, A. Libchaber, and M. Shelley, Nature (London) **408**, 835 (2000).
[19] B. S. H. Connell and D. K. P. Yue, J. Fluid Mech. **581**, 33 (2007).
[20] S. Li and H. Lipson, *Proceedings of ASME Conference on Smart Materials, Adaptive Structures and Intelligent Systems* (ASME, Oxnard, CA, 2009), pp. 611–619.
[21] G. Mustafa and A. Ertas, J. Sound Vib. **182**, 393 (1996).
[22] O. Cuvalci and A. Ertas, J. Vibr. Acoust. **118**, 558 (1996).
[23] O. Cuvalci, J. Sound Vib. **229**, 837 (2000).
[24] A. H. Nayfeh and D. T. Mook, J. Mech. Des. **117**, 186 (1995).
[25] S. Alben and M. Shelley, Phys. Rev. Lett. **100**, 074301 (2008).
[26] Z. Wang and Y. Xu, Appl. Phys. Lett. **90**, 263512 (2007).
[27] H. Kim, A. Batra, S. Priya, K. Uchino, D. Markley, R. E. Newnham, and H. F. Hofmann, Jpn. J. Appl. Phys., Part 1 **43**, 6178 (2004).
[28] C.-T. Chen, R. A. Islam, and S. Priya, IEEE Trans. Ultrason. Ferroelectr. Freq. Control **53**, 656 (2006).

Supplemental materials for paper: 076024JAP

Title: Ambient Wind Energy Harvesting using Cross-Flow Fluttering

Authors: Shuguang Li[1, 2], Jianping Yuan[1] and Hod Lipson[2]

Affiliations:

1. College of Astronautics, Northwestern Polytechnical University, Xi'an, Shaanxi, P. R. China

2. Sibley School of Mechanical and Aerospace Engineering, Cornell University, Ithaca, NY, USA

1. Related work

In order to harvest fluid-induced energy, previous work has investigated the use of an "energy harvesting eel" design using Polyvinylidene Fluoride (PVDF), which converts the flow energy in oceans and rivers to electrical power through a flow-induced oscillating motion on the PVDF film behind a bluff body. [11, 12] A flag-like wind energy harvester was also constructed using PVDF with a similar mechanism.[40] Akaydin *et al* placed their short PVDF cantilever harvester inside turbulent boundary layers and the wakes of circular cylinders, however, unlike the traditional design, the free-end of the cantilever was directed upwind.[41, 42] Instead of using PVDF, Pobering *et al* placed PZT cantilevers directly behind a bluff body to harvest flow energy.[43] The Windbelt[15] device employs a tensioned membrane undergoing flutter oscillation that converts mechanical energy into electricity by electromagnetic induction. [38] Priya, Myers *et al* designed and optimized a small windmill prototype that bends a series of piezoelectric bimorphs transducers to extract energy from airflow. [13, 14] A variety of other wind energy generation concepts based on piezoelectric and magnet materials have been also presented. [16, 35, 36, 39, **44**]

2. Configuration of generators

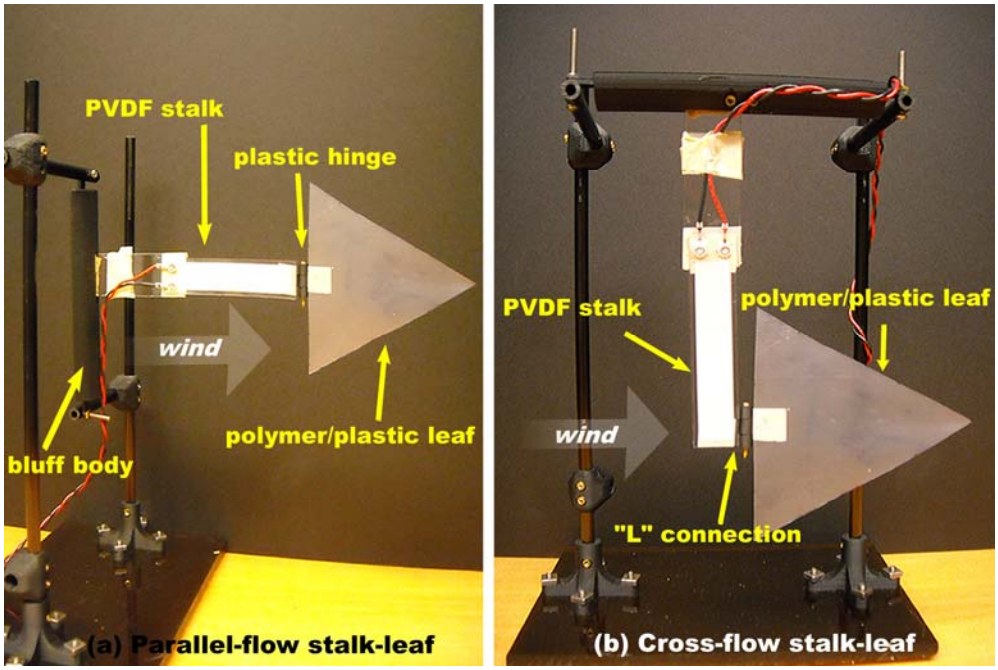

Fig.1. Two wind energy harvesting dangling leaf-stalk configurations: (a) Parallel-flow stalk-leaf. (b) Cross-flow stalk-leaf.

The design of typical parallel-flow stalk leaf is to clamp one edge of PVDF element (LDT2-028K/L w/rivets [18]) to the bluff body as the "stalk" and attach a piece of plastic or polymer film on the downstream end of PVDF stalk as the "leaf". The PVDF stalk is oriented in the direction of airflow (Fig.1a).

In Fig.1.(b), a laminated PVDF element (LDT2-028K/L w/rivets) is clamped in the vertical direction across the airflow, and a triangle shape polymer leaf is attached to the free end of stalk through a pair of small plastic hinges (weight= 0.7g) which were fabricated by using ABS on a 3D-printer (Dimension SST 768; Stratasys Inc).

3. Calculation methods for Table Ⅰ

TABLE Ⅰ: Power density comparison of wind energy harvesting devices

Device	Configuration	Dimension (mm)	Peak power	Power density				Cut-in speed
				per weight (mW/kg)	per volume (mW/cm^3)	per swept area (W/m^2)	per cost (mW/US$)	
Small windmill [a]	bimorph	60 × 20 × 0.6	5mW	77.2	0.579	0.13	0.021	2.4m/s
Galloping beam [b]	bimorph	100 × 38 × 1.54	1.14mW	74	0.556	Unknown	Unknown	2.5m/s
Windbelt (micro)[c,d]			5mW	Unknown	Unknown	1.28	Unknown	2.7m/s
Tan's Harvester [e]	bimorph	76.7 × 12.7 × 2.2	0.16mW	9.94	0.075	Unknown	Unknown	~3 m/s
Flag-like Harvester [h]	bimorph	203 × 279 × 0.5	10mW	Unknown	0.347	Unknown	0.033	~4.5 m/s
Devices presented in this paper								
Parallel-flow long-stalk [f]	unimorph	72 × 16 × 0.205	0.02mW	34	0.09	0.001	0.003	1.5m/s
Cross-flow long-stalk	unimorph	72 × 16 × 0.205	0.21mW	343	0.871	0.013	0.034	1.5m/s
Cross-flow Short-stalk	unimorph	41 × 16 × 0.205	0.26mW	576	1.928	0.046	0.069	4m/s
Cross-flow Double-layers-long stalk	bimorph	72 × 16 × 0.41	0.61mW	472	1.300	0.039	0.051	4m/s
Cross-flow Narrow-short stalk	unimorph	41 × 8 × 0.205	0.14mW	415	2.036	0.024	0.037	2.8m/s
Typical commercial wind turbine								
VESTAS V52-850KW [g]			850 KW	27,000	Unknown	400	~300	4m/s

[a] Reference 14.

[b] Reference 36.

[c] Reference 15.

[d] Reference 38.

[e] Reference 39.

[f] Reference 26.

[g] Reference 37.

[h] Reference 40.

[i] The weight and volume are of piezo-element used in device; for wind turbine, the weight counts the rotor's weight (~10 ton);

[j] Because of insufficient published data, we use approximate density of PZT (7500 kg/m^3) to estimate weights of previous devices; for our devices, the weight is 0.6, 0.45, 1.3 and 0.33 (×10^{-3} kg) as the

sequence order in the table respectively;

[k] Compared to "windmill" and wind-turbine, we use half round as approximate swept area for our devices, the radius is the devices' length, long stalk ~10cm and short stalk ~6cm respectively;

[l] The prices of materials are based on official quotations;

[m] All data in table are within ± 6% error range of measurement and calculation.

4. Experimental results on "optimal resistance"

When measuring power, the load can greatly affect the results. Previous research suggested an optimized matching resistance for output power of piezoelectric based vibration generator, R_0. When neglecting dielectric loss factor and damping, [5, 12, 33, 34] it could be approximately given as:

$$R_o = \frac{1}{2\pi fC}, \tag{1}$$

Where f is the frequency of vibration, and C is the capacitance of the piezoelectric element. We validated this in two experiments on a short stalk and a narrow-short stalk, as Fig. a, b shows. We approached the peak values around the theoretically optimal values in both cases.

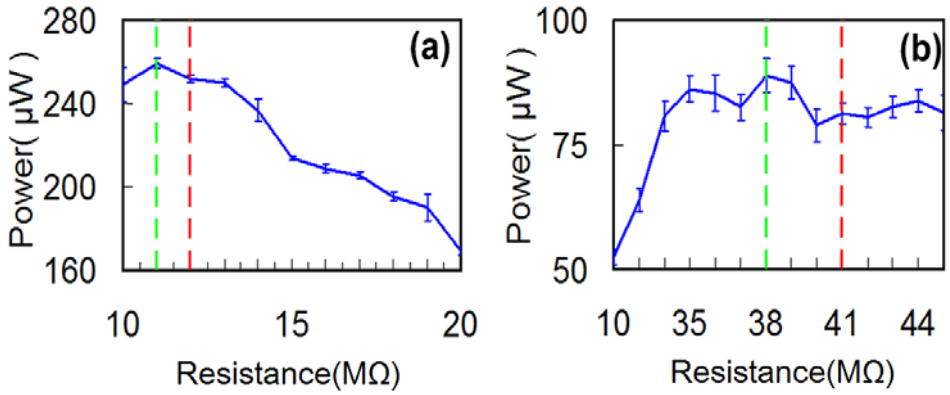

Fig. 2. Output power with different loads: green lines indicate peak values in experiments and red lines are theoretically optimal values. (a) Using a short-stalk (capacitance~1.38nF, see reference 18) with 0.01" PEEK equilateral triangle leaf (hemline=10cm) tests at wind speed about 8 m/s (flapping frequecy~9.4 HZ); (b) Using a narrow-short-stalk (capacitance~0.69nF) with same leaf as in (a), validates at wind speed about 5.6 m/s (flapping frequecy~5.6 HZ).

5. The simplified system model and its explanation on experimental results

When constructing a system model, we ideally assume the system is conservative, implying no dissipation of system energy by damping and friction; we also consider the leaf in pure bending and materials with liner elastic properties. We also ignored the kinetic energy of the stalk. An aero-elastic coupled system from an energy perspective represents wind-induced work to be equal to the total energy within the coupled system as:

$$E_w = \frac{\sigma^2}{2Y} V + \frac{1}{2} J\omega^2 + U_S \,, \tag{2}$$

Where the term of E_W is external works done by wind; $(J\omega^2)/2$ represents the

kinetic energy of the flapping leaf, in which J is moment of inertia, ω is the angular speed of flapping leaf; $(\sigma^2 V)/2Y$ and U_S denote the elastic potential energy (strain energy) of the leaf and piezo-stalk respectively, σ represents the point stress of the leaf, Y is the young's modulus of leaf's materials and V represents the volume of leaf. Based on the equation, we could roughly analyze the qualitative trends of output power. As the increasing of Y and the decreasing of J (which is in direct proportion to materials' density) on the leaf's materials, the stalk's strain energy term, U_S, could become more proportional to the total external work E_W. This would imply that more potential energy will be available for converting to electrical energy. This trend is obvious during the low wind speed region (≤5m/s) and with some exceptions over other regions, as shows in Fig.d. Three reasons should be responsible for this: firstly, with the increasing of wind speed, the friction and damping will dissipate more energy; second, torsion modes emerge and the pure bending models are no longer representative; third, the ignored term of stalk's kinetic energy is becoming more significant.

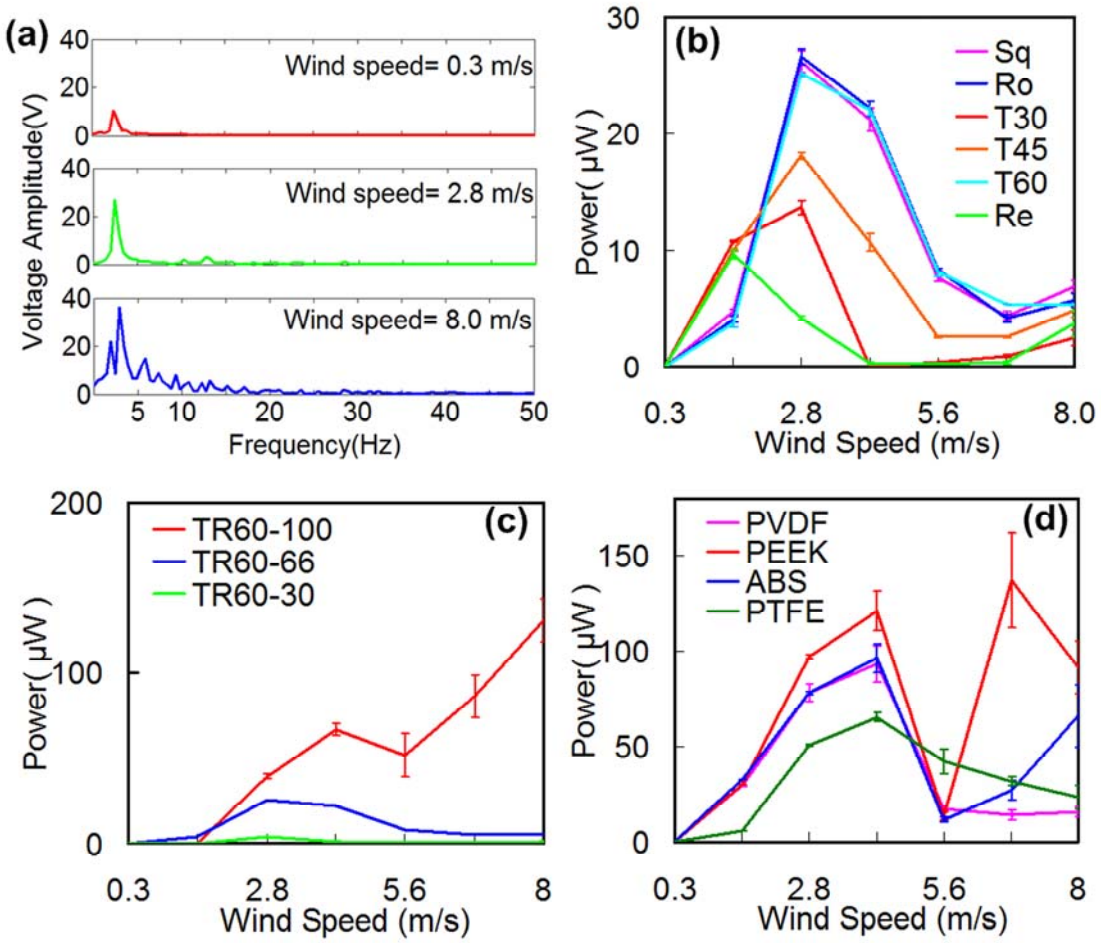

Fig.3. Leaf performance: (a) Typical wind response of piezo-leaf's output, where the red plot is a bi-stable status, green plot has single stable status and blue plot is a chaotic multiple-modals oscillation/bi-stable response. (b) Output power on different shapes of leaf with same materials (PVDF with 0.01" thickness) and area(14.4 cm^2), where Sq, Ro, T30, T45, T60 and Re denotes shape of square, round, isosceles triangle (30 degree base angle), isosceles triangle (45 degree base angle), equilateral triangle and rectangle (7.2 X 2 cm) respectively. (c) Output power on same materials(PVDF with 0.01" thickness) and shapes(equilateral triangle) of leaf but different areas red, blue and green lines represent the hemline's length on 10, 6.6, 3 cm respectively. (d) Different materials' output power using same shape (equilateral

triangle) and area (hemline=10 cm); materials' properties [young's modulus (MPa), density (kg/m^3)] as follows: PVDF [2100-2900, 1780], PEEK [3700, 1320], ABS [2300, 1070] and PTFE [410-750, 2175].

References:

[1] S. R. Anton and H. A. Sodano, Smart Mater. Struct. 16, R1 (2007).

[2] 2J. A. Paradiso and T Starner, IEEE Pervasive Comput. 4, 18(2005).

[3] H. A. Sodano, D. J. Inman, and G. Park, Shock Vib. Dig. 36, 197 (2004).

[4] S. P. Beeby, M. J. Tudor and N. M. White, Meas. Sci.Technol. 17, R175(2006).

[5] S. Priya, J. Electroceram. 19,167(2007).

[6] S. Roundy, P. K. Wright and J. Rabaey, Comput.Commun.26, 1131(2003).

[7] D. Shen, S. Choe and D. Kim, Jpn. J. Appl. Phys. 46, 6755(2007).

[8] H. A. Sodano, G. Park and D. J. Inman, Strain, 40(2), 49(2004).

[9] A. Erturk, J. Hoffmann, and D. J. Inman, Appl. Phys. Lett. 94, 254102(2009).

[10] F. C. Moon and P. J. Holmes, J. Sound Vib. 65, 275 (1979).

[11] G. W. Taylor, J. R. Burns, S. M. Kammann, W. B. Powers, and T. R. Welsh, IEEE J. Ocean. Eng. 26, 539(2001).

[12] J. J. Allen and A. J. Smits, J. Fluids Struct. 15, 629(2001).

[13] S. Priya, Appl. Phys. Lett. 87, 184101(2005).

[14] R. Myers, M. Vickers, H. Kim, and S. Priya, Appl. Phys. Lett. 90, 054106 (2007).

[15] L. Ward, Popular Mechanics.30 Jan, (2008).

[16] R.M. Dickson, New Concept in Renewable Energy, (2008)

[17] C. H. K. Williamson and R Govardhan, Annu. Rev. Fluid Mech. 36, 413(2004).

[18] Measurement Specialties. Inc, Piezo Film Product Guide and Price List, (2008).

[19] S. Shukla, R.N. Govardhan and J.H. Arakeria, J. Fluids Struct. 25, 713(2009)

[20] L. Huang, J. Fluids Struct. 15, 127(1995).

[21] M Argentina and L Mahadevan, Proc. Natl. Acad. Sci. U.S.A. 102, 1829 (2005).

[22] L. Tang and M. P. Païdoussis, J. Sound Vib. 305, 97(2007).

[23] C. Eloy, C. Souilliez and L. Schouveiler, J. Fluids Struct. 23, 904(2007).

[24] J. Zhang, S. Childress, A. Libchaber and M. Shelley, Nature. 408, 835(2000).

[25] B. S. H. Connell and D. K. P. Yue, J. Fluid Mech. 581, 33(2007).

[26] S. Li and H. Lipson, Proc. ASME Conference on Smart Materials, Adaptive Structures and Intelligent Systems, (ASME, Oxnard, CA, 2009), pp. 611-619.

[27] G. Mustafa and A. Ertas, J. Sound Vib. 182, 393(1996).

[28] O. Cuvalci and A. Ertas, J. Vib. Acoust. 118, 558(1996).

[29] O. Cuvalci, J. Sound Vib. 229,837(2000).

[30] A. H. Nayfeh and D. T. Mook, J. Mech. Des. 117, 186(1995).

[31] S. Alben and M. Shelley, Phys. Rev. Lett. 100, 074301 (2008).

[32] Z. Wang and Y. Xu, Appl. Phys. Lett. 90, 263512 (2007).

[33] H Kim, A. Batra, S. Priya, K. Uchino, D. Markley, R. E. Newnham, and H. F. Hofmann, Jpn. J. Appl. Phys. 43, 6178(2004).

[34] C. Chen, R. A. Islam and S. Priya, IEEE Trans. Ultrason. Ferroelectr. Freq. Control. 53, 656(2006).

[35] M. Bryant and E. Garcia, Proc. SPIE, 7288, 728812 (2009).

[36] R. R. Mahadik and J. Sirohi, Proc. ASME Conference on Smart Materials, Adaptive Structures and Intelligent Systems, (ASME, Oxnard, CA, 2009), pp. 443-450.

[37] Vestas Wind Systems A/S, Wind Turbine Products' Brochures of V52-850 kW.

[38] MicroBelt tech sheet, http://www.humdingerwind.com/

[39] Y. K. Tan and S. K. Panda, Proc. Annu. Conf. IEEE Ind. Electron. Soc. (IEEE, Taipei, 2007), pp. 2175-2180.

[40] W. P. Robbins, I. Marusic, D. Morris, and T. O. Novak, Proc. ASME International Mechanical Engineering Congress and Exposition, (ASME, Chicago, IL, 2006), pp. 581-590.

[41] H. D. Akaydin, N. Elvin, and Y. Andreopoulos, J. Intell. Mater. Struct. 0, 1(2010).

[42] H. D. Akaydin, N. Elvin, and Y. Andreopoulos, Exp. Fluids. (2010).

[43] S. Pobering, S. Ebermeyer and N. Schwesinger, Proc. SPIE, 7288, 728807 (2009).

[44] N. S. Hudak and G. G. Amatucci, J. Appl. Phys. 103, 101301(2008).